

New Hybrid Variational Recovery Model for Blurred Images with Multiplicative Noise

Yiqiu Dong¹ and Tieyong Zeng^{2,*}

¹ Department of Applied Mathematics and Computer Science, Technical University of Denmark, Denmark.

² Department of Mathematics, Hong Kong Baptist University, Kowloon Tong, Hong Kong.

Received 24 July 2013; Accepted (in revised version) 12 August 2013

Available online 28 November 2013

Abstract. A new hybrid variational model for recovering blurred images in the presence of multiplicative noise is proposed. Inspired by previous work on multiplicative noise removal, an I-divergence technique is used to build a strictly convex model under a condition that ensures the uniqueness of the solution and the stability of the algorithm. A split-Bregman algorithm is adopted to solve the constrained minimisation problem in the new hybrid model efficiently. Numerical tests for simultaneous deblurring and denoising of the images subject to multiplicative noise are then reported. Comparison with other methods clearly demonstrates the good performance of our new approach.

AMS subject classifications: 52A41, 65K05, 65K15, 90C25, 90C30

Key words: Convex model, image deblurring, multiplicative noise, Split-Bregman Algorithm, total variation, variational model.

1. Introduction

Image restoration is a classical and important inverse problem in imaging science. In past decades, many restoration methods have been developed for this task — cf. [4, 11, 15, 33, 39, 46] and references therein. In this article, we consider the restoration of blurred images that are also corrupted by multiplicative noise.

Suppose that an image \hat{u} is a real function defined on Ω , a connected bounded open subset of \mathbb{R}^2 with compact Lipschitz boundary — i.e. $\hat{u} : \Omega \rightarrow \mathbb{R}$. The degraded image f in the presence of simultaneous blurring and multiplicative noise can be represented as

$$f = (A\hat{u})\eta , \quad (1.1)$$

where f is positive, $A \in \mathcal{L}(L^2(\Omega))$ is a known bounded linear operator, and η denotes a multiplicative noise with mean one. Multiplicative noise commonly appears in real

*Corresponding author. Email addresses: yido@dtu.dk (Y. Dong), zeng@hkbu.edu.hk (T. Zeng)

applications such as laser images, ultrasound imaging, synthetic aperture radar (SAR), etc. [5, 38, 42, 44]. Here we specifically focus on multiplicative Gamma noise — i.e. where η follows a Gamma distribution [2, 30]. Compared with the denoising case where A is the identity operator, the deblurring poses some extra challenges. This is because image deblurring is an ill-posed problem, due to either the possible nonuniqueness of the solution or numerical instability induced by the operator A [15]. In order to overcome these problems, several variational models with regularisation have been proposed, based on the image degradation model and prior information on \hat{u} .

Indeed, according to the statistical properties of η , the recovery of the image \hat{u} may be achieved by solving the constrained minimisation problem [38]

$$\begin{aligned} & \inf_{u \in S(\Omega)} \int_{\Omega} |Du| \\ & \text{subject to } \int_{\Omega} f / (Au) dx = 1 \text{ and } \int_{\Omega} [f / (Au) - 1]^2 dx = \theta^2, \end{aligned} \quad (1.2)$$

where θ is the standard deviation of η and $S(\Omega) = \{v \in BV(\Omega) : v > 0\}$. Here $BV(\Omega)$ denotes the space of functions of bounded variation (i.e. $u \in BV(\Omega)$ if and only if $u \in L^1(\Omega)$), and the BV-seminorm

$$\int_{\Omega} |Du| := \sup \left\{ \int_{\Omega} u \cdot \operatorname{div}(\xi(x)) dx : \xi \in C_0^\infty(\Omega, \mathbb{R}^2), \|\xi\|_{L^\infty(\Omega, \mathbb{R}^2)} \leq 1 \right\} \quad (1.3)$$

is finite. The space $BV(\Omega)$ endowed with the norm $\|u\|_{BV} = \|u\|_{L^1} + \int_{\Omega} |Du|$ is a Banach space. If $u \in BV(\Omega)$, the distributional derivative Du is a bounded Radon measure and the term $\int_{\Omega} |Du|$ defined in (1.3) corresponds to the total variation (TV). Based on the compactness of $BV(\Omega)$, in the two-dimensional case one has the embedding $BV(\Omega) \hookrightarrow L^p(\Omega)$ for $1 \leq p \leq 2$, compact for $p < 2$ — cf. [1, 3, 15] for more detail.

In the model (1.2), which we call the RLO model, the TV of u is applied as the objective function in order to preserve edge information in the images. Only basic statistical properties of the noise η (viz. the mean and the variance) are involved in (1.2), which slightly limits the quality of the restored images. Consequently, based on *maximum a posteriori* (MAP) analysis of the multiplicative Gamma noise, Aubert & Aujol [2] proposed the following variational model for image deblurring under multiplicative noise, which we refer to as the AA model:

$$\inf_{u \in S(\Omega)} \int_{\Omega} \left(\log(Au) + \frac{f}{Au} \right) dx + \lambda \int_{\Omega} |Du|, \quad (1.4)$$

where the TV of u is again used as the regularisation term and $\lambda > 0$ is the regularisation parameter that controls the trade-off between a good fit of f and smoothness due to the TV regularisation. Since both the RLO model (1.2) and the AA model (1.4) are non-convex, the gradient projection algorithms proposed in Refs. [2, 38] may lead to certain local minimisers, so the quality of the corresponding restoration results is strongly dependent on the initial estimations of \hat{u} and the numerical optimisation procedures used.

For multiplicative noise removal in (1.4), Huang *et al.* [29] recently suggested that an auxiliary variable $z = \log u$ be used, and Shi *et al.* [42] added an extra quadratic term. Both initiatives produced convex models, such that the denoising results are independent of the initialisations. In addition, Steidl *et al.* [43] combined the I-divergence term with the TV or nonlocal means regularisation, for multiplicative Gamma noise removal. In Ref. [20], the multiplicative noise removal task was approached by applying an L^1 -data-fitting term on the frame coefficients. However, none of these developments addressed the image restoration problem in the simultaneous presence of blurring.

In this article, we consider the restoration of images that are distorted by some blurring operator in the presence of multiplicative Gamma noise. Although the AA model (1.4) is based on MAP analysis of the multiplicative Gamma noise, the model non-convexity revokes uniqueness and convergence in the numerical solution. Given the success of the I-divergence technique in multiplicative noise removal [43], we combine that technique with the data-fitting term from MAP analysis in the context of (1.4), and propose a new hybrid model that is convex under a mild condition. The existence and uniqueness of a solution under the new hybrid model on continuous spaces are then considered. Here the TV regularisation is applied to preserve edges during the reconstruction, and it can be readily replaced by some modern regularisation terms — e.g. non-local TV [24, 47], the framelet approach [11], etc. The minimisation problem in our model is solved by the split-Bregman algorithm [10], instead of the gradient projection method used in Refs. [2, 38]. The numerical results indicate that our method outperforms both the RLO model [38] and the AA model [2], with respect to both image restoration capability and computational efficiency.

In summary, we introduce a superior new convex hybrid model to simultaneously deblur and remove multiplicative Gamma noise. Further, we present a theoretical discussion of this new model — including its convexity, solution existence and uniqueness, comparison theorem and (importantly) bias correction. Together with I-divergence, in Section 2 we discuss multiplicative Gamma noise removal under our new convex hybrid model, including solution existence and uniqueness and several other important properties as mentioned. In Section 3, we extend the model to the general case of simultaneous denoising and deblurring, with the corresponding mathematical properties likewise discussed. In Section 4, we apply the split-Bregman algorithm to solve the optimisation problem in our model, based on the work done previously in Refs. [23, 26]. The numerical results presented in Section 5 show that our new model is indeed a significant advance, and some concluding remarks are made in Section 6.

2. New Hybrid Multiplicative Denoising Model

Let us first consider denoising alone — i.e. where A is the identity operator in (1.1). Furthermore, we assume that the noise η follows a Gamma distribution, as is common in synthetic aperture radar (SAR) for example. We recall that the probability density function

of the Gamma-distributed random variable η is

$$p_\eta(x; \theta, K) = \frac{1}{\theta^K \Gamma(K)} x^{K-1} e^{-x/\theta} \quad \text{for } x \geq 0, \quad (2.1)$$

where Γ is the classical Gamma-function and θ and K denote the scale and shape parameters, respectively. Moreover, the mean of η is $K\theta$, and the variance is $K\theta^2$ [27]. For multiplicative noise, one usually assumes that the mean of η is one (i.e. $K\theta = 1$) and the variance is $1/K$ [2, 20].

The non-convex variational model (1.4) was proposed to remove multiplicative Gamma noise, based on MAP noise analysis [2]. Due to its lack of global convexity, the restored results obtained on solving (1.4) strongly depend upon the initialisation and numerical optimisation procedures adopted. To overcome this, an I-divergence model was introduced in Ref. [43], where the I-divergence (sometimes called the “generalised Kullback-Leibler divergence” [18]) defined by

$$I(f, u) := \int_{\Omega} \left(f \log \frac{f}{u} - f + u \right) dx$$

was used as the data-fitting term. This corresponds to the Bregman distance of the function $Q(u) := \int_{\Omega} u \log u dx$ — i.e. $I(f, u) = Q(f) - Q(u) - \langle q, f - u \rangle$ with $q \in \partial Q(u)$, as in Ref. [10] except that the choice of $Q(u)$ is slightly different, and so inherits the attractive properties of the Bregman distance (e.g. $I(f, u) \geq 0$). On removing constant terms, the I-divergence model for multiplicative Gamma noise removal may be rewritten as

$$\inf_{u \in S(\Omega)} \int_{\Omega} (u - f \log u) dx + \lambda \int_{\Omega} |Du|, \quad (2.2)$$

where $\lambda > 0$ is the regularisation parameter. Significantly, this reduced model (2.2) is convex. Although the data-fitting term $\int_{\Omega} (u - f \log u) dx$ in (2.2) is somewhat more closely related to Poisson noise according to MAP analysis [34], this model is also successful in removing multiplicative Gamma noise [43]. Given the perceived advantages and disadvantages of (1.4) and (2.2), we have been led to propose the following new hybrid multiplicative denoising model.

2.1. Our new model

In order to retain both the outcome from MAP analysis of the Gamma noise and convexity from the I-divergence, we introduce the following hybrid multiplicative denoising model:

$$\inf_{u \in \bar{S}(\Omega)} E(u) := \int_{\Omega} \left(\log u + \frac{f}{u} \right) dx + \alpha \int_{\Omega} (u - f \log u) dx + \lambda \int_{\Omega} |Du|, \quad (2.3)$$

where the parameter $\alpha > 0$ and $\bar{S}(\Omega) := \{v \in BV(\Omega) : v \geq 0\}$ is a closed convex set. In addition, we define $\log 0 = -\infty$ and $1/0 = +\infty$.

The parameter α in (2.3) controls the balance of the first two terms. Thus if α is small and close to 0, (2.3) approximates the non-convex AA model (1.4); and conversely, the I-divergence term dominates in the first two terms if α is sufficiently large, so (2.3) tends to the convex I-divergence model (2.2). Moreover, there is the interesting possibility that not only may α be chosen small enough to retain relevance to the Gamma distribution, but also big enough to overcome the non-convexity shortcoming of (1.4). In the following section, we obtain such a moderate value for the parameter α , and discuss the existence and uniqueness of the corresponding solution to (2.3).

2.2. General Bregman distance model

Before discussing the mathematical properties of our new model (2.3), we make an interesting observation. For an arbitrary function $Q(u)$, on defining the Bregman distance

$$I_Q(f, u) := Q(f) - Q(u) - \langle q, f - u \rangle$$

with $q \in \partial Q(u)$ we can consider a general Bregman distance model — viz.

$$\inf_u I_Q(f, u) + \lambda \int_{\Omega} |Du| . \quad (2.4)$$

Ignoring any constant term, this model reduces to: (1) the TV model for Gaussian noise removal [39] when $Q(u) = \int_{\Omega} u^2 dx$; (2) the AA model when $Q(u) = \int_{\Omega} -\log u dx$; and (3) the I-divergence model [43] when $Q(u) = \int_{\Omega} u \log u dx$. Moreover, if we choose $Q(u) = \int_{\Omega} (-\log u + \alpha u \log u) dx$, (2.4) becomes our hybrid model (2.3).

2.3. Solution existence and uniqueness

To investigate the existence and uniqueness of a solution to (2.3), we start by discussing the convexity of the model. The I-divergence term provides additional convexity, and we can prove that $E(u)$ defined in (2.3) is strictly convex if the parameter α satisfies a certain condition as follows.

Proposition 2.1. *If $\alpha \geq 1/\inf_{\Omega} f > 0$, then the model (2.3) is strictly convex.*

Proof. For a fixed $x \in \Omega$, we define a function $g(t) \in \mathbb{R}^+$ with a given α as

$$g(t) := \log t + \frac{f(x)}{t} + \alpha (t - f(x) \log t) .$$

The second derivative of this function is

$$g''(t) = (\alpha f(x) - 1)t^{-2} + 2f(x)t^{-3} ,$$

hence if $\alpha \geq 1/\inf_{\Omega} f$ then $g''(t) > 0$ — i.e. g is strictly convex.

Now considering all $x \in \Omega$, we have strict convexity of the first two terms in (2.3); and

given the convexity of the TV regularisation, we deduce that $E(u)$ in (2.3) is strictly convex if $\alpha \geq 1/\inf_{\Omega} f$. Since the feasible set $\bar{S}(\Omega)$ is convex, the assertion follows immediately. \square

With this convexity result, we have the following theorem on the existence and uniqueness of a solution to the model (2.3), and also a maximum principle.

Theorem 2.1. *Let f be in $L^{\infty}(\Omega)$ with $\inf_{\Omega} f > 0$. Then the model (2.3) has a solution u^* in $\bar{S}(\Omega)$, satisfying*

$$0 < \inf_{\Omega} f \leq u^* \leq \sup_{\Omega} f .$$

Moreover, if $\alpha \geq 1/\inf_{\Omega} f$, the solution of (2.3) is unique.

A proof of this theorem is readily realised under Theorem 4.1 in Ref. [2]. In particular, if $\alpha \geq 1/\inf_{\Omega} f$ the uniqueness follows directly from the strict convexity of the function E .

In Ref. [2], a comparison principle was given for the model (1.4), and this principle remains valid for (2.3) as follows.

Proposition 2.2. *Let f_1 and f_2 be in $L^{\infty}(\Omega)$ with $\inf_{\Omega} f_1 > 0$ and $\inf_{\Omega} f_2 > 0$. Assume that $f_1 < f_2$. Suppose that u_1^* (respectively u_2^*) is a solution of (2.3) with $f = f_1$ (respectively $f = f_2$). Then $u_1^* \leq u_2^*$.*

The proof of this proposition for (2.3) has a structure similar to the proof of Proposition 4.3 in Ref. [2]. Except for the uniqueness of the solution, the results in Theorem 2.1 and Proposition 2.2 do not depend on the selection of α , hence they also hold for the I-divergence model (2.2). Moreover, since the objective function of the model (2.2) is strictly convex, uniqueness is straightforward. The extension to the general model (2.4) under a mild condition is also possible, but we leave the relevant details to interested readers.

3. New Hybrid Model for Simultaneous Deblurring and Denoising

During acquisition and transmission, images are commonly blurred and corrupted by noise, and we now return to simultaneous deblurring and denoising. We consider the model (2.3) for multiplicative Gamma noise removal, and based on the statistical properties of the Gamma distribution proceed to encompass simultaneous deblurring and denoising — i.e. we seek to restore the image \hat{u} in (1.1) subject to the blurring operator A and Gamma noise in (2.3). The restoration proceeds via the constrained minimisation problem

$$\inf_{u \in \bar{S}(\Omega)} E_A(u) := \int_{\Omega} \left(\log(Au) + \frac{f}{Au} \right) dx + \alpha \int_{\Omega} (Au - f \log(Au)) dx + \lambda \int_{\Omega} |Du| , \quad (3.1)$$

where $A \in \mathcal{L}(L^2(\Omega))$ is a known bounded linear operator. Since it is a blurring operator, we assume that A is nonnegative (i.e. $A \geq 0$) such that $Au \geq 0$ where $u \in \bar{S}(\Omega)$. As in Proposition 2.1, since A is linear we can readily establish the following convexity result.

Proposition 3.1. *If $\alpha \geq 1/\inf_{\Omega} f$, then the model (3.1) is convex. Furthermore, if A is also injective, then (3.1) is strictly convex.*

3.1. Solution existence and uniqueness

From the properties of the space of bounded variation functions and total variation, we prove the following existence and uniqueness result for (3.1).

Theorem 3.1. *Suppose that $A \in \mathcal{L}(L^2(\Omega))$ is nonnegative, and it does not annihilate constant functions — i.e. $A1 \neq 0$. If $f \in L^\infty(\Omega)$ satisfies $\inf_\Omega f > 0$, then the model (3.1) admits a solution u^* . Moreover, if $\alpha \geq 1/\inf_\Omega f$ and A is injective, then the solution is unique.*

Proof. Since E_A is bounded from below, we choose a minimising sequence $\{u_n\} \in \bar{S}(\Omega)$ for (3.1) with $n = 1, 2, \dots$, so $\{\int_\Omega |Du_n|\}$ is bounded. Recalling that Ω is bounded, based on the Poincaré inequality (cf. Remark 3.50 in Ref. [1]) we obtain

$$\|u_n - m_\Omega(u_n)\|_2 \leq C \int_\Omega |D(u_n - m_\Omega(u_n))| = C \int_\Omega |Du_n|, \quad (3.2)$$

where $m_\Omega(u_n) = \int_\Omega u_n dx / |\Omega|$ involves $|\Omega|$ denoting the measure of Ω and C is a constant depending only on Ω . Consequently, $\|u_n - m_\Omega(u_n)\|_2$ is bounded for each n . According to the continuity of the operator A , $\{A(u_n - m_\Omega(u_n))\}$ must be uniformly bounded in $L^2(\Omega)$ and in $L^1(\Omega)$.

As $\{u_n\}$ is a minimisation sequence, it is not difficult to check that $\|Au_n\|_1$ is bounded. Indeed, since both

$$\int_\Omega \left(\log(Au_n) + \frac{f}{Au_n} \right) dx \quad \text{and} \quad \int_\Omega [Au_n - f \log(Au_n)] dx$$

are uniformly bounded for $x \in \Omega$, if we define

$$g_n(x) := \begin{cases} \sup_\Omega f, & \text{if } Au_n(x) \geq 1, \\ \inf_\Omega f, & \text{otherwise,} \end{cases}$$

then g_n is measurable and therefore

$$\int_\Omega g_n(x) \cdot \left(\log(Au_n) + \alpha \frac{f}{Au_n} \right) dx + \int_\Omega (Au_n - f \log(Au_n)) dx$$

is uniformly bounded. For any $x \in \Omega$,

$$(g_n(x) - f(x)) \log(Au_n(x)) \geq 0 \quad \text{and} \quad g_n(x) \cdot \frac{f(x)}{Au_n(x)} > 0,$$

so we immediately have that $\int_\Omega Au_n dx$ — i.e. $\|Au_n\|_1$ is uniformly bounded. Since

$$|m_\Omega(u_n)| \cdot \|A1\|_1 = \|A(u_n - m_\Omega(u_n)) - Au_n\|_1 \leq \|A(u_n - m_\Omega(u_n))\|_1 + \|Au_n\|_1,$$

we have that $|m_\Omega(u_n)| \cdot \|A1\|_1$ is uniformly bounded, and thus $m_\Omega(u_n)$ is uniformly bounded since $A1 \neq 0$. Together with the boundedness of $\{u_n - m_\Omega(u_n)\}$, this implies the boundedness of $\{u_n\}$ in $L^2(\Omega)$ and thus in $L^1(\Omega)$. Since $\bar{S}(\Omega)$ is closed and convex, $\{u_n\}$ is also bounded in $\bar{S}(\Omega)$.

Consequently, a subsequence $\{u_{n_k}\}$ exists that converges weakly in $L^2(\Omega)$ to some $u^* \in L^2(\Omega)$, and $\{Du_{n_k}\}$ converges weakly as a measure to Du^* . Given continuity of the linear operator A , it follows that $\{Au_{n_k}\}$ converges weakly to Au^* in $L^2(\Omega)$. Then from the lower semi-continuity of the total variation and Fatou's lemma, we have that u^* is a solution of the model (3.1). From Proposition 3.1, when $\alpha \geq 1/\inf_\Omega f$ and A is injective the model (3.1) is strictly convex, so its solution is unique. \square

Remark 3.1. In the proof of Theorem 3.1, with the α -term we obtain the boundedness of the sequence $\{Au_n\}$ in $L^1(\Omega)$. However, when $\alpha = 0$ — i.e. in the model (1.4) — it is difficult to get the same result, so in the continuous case the proof of existence of a solution to (1.4) remains an open question.

Because of the constraint $u \in \bar{S}(\Omega)$, the solution of (3.1) is nonnegative. Further, we have the following result.

Proposition 3.2. *Suppose that u^* is a solution of (3.1), and define $C_1 = E_A(u^*)$. Then for any $0 < \epsilon < 1$,*

$$|\{x \in \Omega : Au^*(x) \leq \epsilon f(x)\}| \leq \frac{\epsilon}{1 + \epsilon \log \epsilon} \left(C_1 - \int_\Omega (\log f - \alpha f \log f + \alpha f) dx \right).$$

Proof. Based on the definition of TV in (1.3), the TV of u^* is nonnegative, so we obtain

$$\int_\Omega \left(\log w + \frac{1}{w} \right) dx + \alpha \int_\Omega f(w - \log w) dx + \int_\Omega (\log f - \alpha f \log f) dx \leq C_1$$

with $w = Au^*/f$. For any $t > 0$, $t - \log t \geq 1$ so that

$$\int_\Omega \left(\log w + \frac{1}{w} \right) dx + \int_\Omega (\log f - \alpha f \log f + \alpha f) dx \leq C_1.$$

Moreover, $\log t + t^{-1} > 0$ for any $t > 0$; and if $0 < t \leq \epsilon < 1$, then $\log t + t^{-1} \geq \log \epsilon + \epsilon^{-1}$. From these two inequalities, we readily obtain

$$|\{x \in \Omega : w(x) \leq \epsilon\}| \leq \frac{\epsilon}{1 + \epsilon \log \epsilon} \left(C_1 - \int_\Omega (\log f - \alpha f \log f + \alpha f) dx \right),$$

such that with $w = Au^*/f$ we arrive at the assertion. \square

It follows that $|\{x \in \Omega : Au^*(x) = 0\}| = 0$ (i.e. $Au^* > 0$ almost everywhere in Ω); and moreover, in the discrete case Au^* is strictly positive — cf. also the results in Ref. [30].

3.2. Bias correction

When TV regularisation was proposed in Ref. [39], the problem of Gaussian noise removal was investigated. Based on MAP analysis of the Gaussian distribution, the L^2 -data-fitting term $\int_\Omega |Au - f|^2 dx$ was combined with TV regularisation in the restoration

model. Theoretical analysis showed that the mean value of the image f is preserved by the solution u^* automatically in this case [13, 15] — i.e.

$$\int_{\Omega} Au^* dx = \int_{\Omega} f dx . \quad (3.3)$$

However, several known models for multiplicative noise removal (including the AA and RLO models) do not have the property (3.3). In Ref. [20], a bias correction step for multiplicative noise removal was consequently proposed, and we now consider this for our new hybrid model (3.1).

Proposition 3.3. *Suppose that $A1 = 1$, and let u^* be a solution of (3.1). Then the following equality holds:*

$$\int_{\Omega} \left(\frac{1}{Au^*} + \alpha \right) \left(1 - \frac{f}{Au^*} \right) dx = 0 .$$

Proof. We define a function with a single non-negative variable $t \in \mathbb{R}$ ($t \geq 0$) — viz.

$$\begin{aligned} e(t) := & \int_{\Omega} \left(\log(A(u^* + t)) + \frac{f}{A(u^* + t)} \right) dx + \alpha \int_{\Omega} [A(u^* + t) - f \log(A(u^* + t))] dx \\ & + \lambda \int_{\Omega} |D(u^* + t)| . \end{aligned}$$

For $A1 = 1$, we necessarily have

$$\begin{aligned} e(t) = & \int_{\Omega} \left(\log(Au^* + t) + \frac{f}{Au^* + t} \right) dx + \alpha \int_{\Omega} [Au^* + t - f \log(Au^* + t)] dx \\ & + \lambda \int_{\Omega} |Du^*| . \end{aligned}$$

Since $t = 0$ is a (local) minimiser of $e(t)$, we have $e'(0) = 0$ such that

$$\int_{\Omega} \left(\frac{1}{Au^*} + \alpha \right) \left(1 - \frac{f}{Au^*} \right) dx = 0 . \quad \square$$

Proposition 3.3 indicates that for our hybrid model (3.1) the property (3.3) is also not met — i.e. in general the mean value of the original image is not automatically preserved. To reduce the influence from the bias and keep the restored image in the same scale as f , we improve the model (3.1) by adding a constraint $m_{\Omega}(u) = m_{\Omega}(f)$ — i.e.

$$\inf_{\{u \in \bar{S}(\Omega) : m_{\Omega}(u) = m_{\Omega}(f)\}} \int_{\Omega} \left(\log(Au) + \frac{f}{Au} \right) dx + \alpha \int_{\Omega} [Au - f \log(Au)] dx + \lambda \int_{\Omega} |Du| . \quad (3.4)$$

In deriving the constraint $m_{\Omega}(u) = m_{\Omega}(f)$ here, we implicitly use (1.1), and the property that $\mathbb{E}(X \cdot Y) = \mathbb{E}(X) \cdot \mathbb{E}(Y)$ if the random variables X, Y are independent. Moreover, it is straightforward to show that the feasible set $\{u \in \bar{S}(\Omega) : m_{\Omega}(u) = m_{\Omega}(f)\}$ is closed and convex, and that the existence and uniqueness results of (3.4) are obtained by extending Theorem 3.1.

4. The Split-Bregman Algorithm for Solving the Improved Model

Because of the convexity, many methods can be used for the minimisation problem in solving the improved model (3.4). For example, the primal-dual algorithm [6, 7, 14, 22, 37] can readily be adapted to various non-smooth convex optimisation problems and it is easy to implement; the alternating direction method [9, 23] is convergent and well-suited to large-scale convex problems; and the split-Bregman algorithm [23, 26, 40, 41, 45] is widely used to solve the L^1 regularisation problems, including TV regularisation. As observed in Ref. [40], the alternating split Bregman algorithm coincides with the alternating direction method of multipliers, which is a special augmented Lagrangian method. In this article, we extend the split-Bregman algorithm to solve the minimisation problem in (3.4).

In the discrete version of (3.4), for simplicity we retain the notation from the continuous context. Suppose that the original image $f \in \mathbb{R}^n$ ($f > 0$) is obtained from a two-dimensional pixel array by concatenation in the usual column-wise fashion, where n is the number of pixels. We denote $\bar{\mathcal{S}} = \{v \in \mathbb{R}^n : v \geq 0\}$ and $\bar{\mathcal{S}}^0 = \{v \in \mathbb{R}^n : v \geq 0, \text{ and } \sum_{i=1}^n v_i = \sum_{i=1}^n f_i\}$, and define the function $G : \bar{\mathcal{S}} \rightarrow \mathbb{R} \cup \{+\infty\}$ as

$$G(v) := \sum_{i=1}^n \left(\log v_i + \frac{f_i}{v_i} \right) + \alpha \sum_{i=1}^n (v_i - f_i \log v_i).$$

Then the discrete version of the model (3.4) reads as follows:

$$\min_{u \in \bar{\mathcal{S}}^0} E_A(u) := G(Au) + \lambda \|\nabla u\|_1, \quad (4.1)$$

where $A \in \mathbb{R}^{n \times n}$ has nonnegative elements and the gradient operator is a map $\nabla : \mathbb{R}^n \rightarrow \mathbb{R}^{2n}$ defined as

$$\nabla v = \begin{bmatrix} \nabla_x v \\ \nabla_y v \end{bmatrix}$$

for $v \in \mathbb{R}^n$, with ∇_x and $\nabla_y \in \mathbb{R}^{n \times n}$ the respective discrete derivative in the x -direction and y -direction. In our numerics, ∇_x and ∇_y are obtained by applying finite difference approximations for the derivatives with symmetric boundary conditions. In addition, $\|\nabla v\|_1$ denotes the discrete total variation of v — i.e.

$$\|\nabla v\|_1 = \sum_{i=1}^n \sqrt{(\nabla_x v)_i^2 + (\nabla_y v)_i^2}.$$

We introduce two new variables w and q , and formulate the corresponding constrained optimisation problem

$$\min_{u \in \bar{\mathcal{S}}^0, w \in \bar{\mathcal{S}}, q \in \mathbb{R}^{2n}} G(w) + \lambda \|q\|_1 \text{ such that } w = Au \text{ and } q = \nabla u,$$

which can be solved by the augmented Lagrangian method [36]. We consider the unconstrained augmented functional:

$$\mathcal{L}(u, w, b_1, b_2, q) := G(w) + \lambda \|q\|_1 + \frac{1}{2\gamma} \|b_1 + Au - w\|_2^2 + \frac{1}{2\gamma} \|b_2 + \nabla u - q\|_2^2, \quad (4.2)$$

where $b_1 \in \mathbb{R}^n$, $b_2 \in \mathbb{R}^{2n}$, $\|\cdot\|_2$ denotes the l^2 -vector-norm, and $\gamma > 0$ is a given parameter. The split-Bregman algorithm is defined through the iterations:

$$u^{k+1} = \arg \min_{u \in \bar{S}^0} \frac{1}{2\gamma} \|b_1^k + Au - w^k\|_2^2 + \frac{1}{2\gamma} \|b_2^k + \nabla u - q^k\|_2^2, \quad (4.3)$$

$$w^{k+1} = \arg \min_{w \in \bar{S}} G(w) + \frac{1}{2\gamma} \|b_1^k + Au^{k+1} - w\|_2^2, \quad (4.4)$$

$$q^{k+1} = \arg \min_{q \in \mathbb{R}^{2n}} \lambda \|q\|_1 + \frac{1}{2\gamma} \|b_2^k + \nabla u^{k+1} - q\|_2^2, \quad (4.5)$$

$$b_1^{k+1} = b_1^k + Au^{k+1} - w^{k+1}, \quad (4.6)$$

$$b_2^{k+1} = b_2^k + \nabla u^{k+1} - q^{k+1}. \quad (4.7)$$

The convergence analysis of such an alternating direction method is addressed in Refs. [21, 23, 31], and it is notable that (4.4) and (4.5) can be grouped together. Moreover, the updates of the variable b_1 and b_2 in the above algorithm are explicit; and since the objective function of (4.3) is quadratic, the solution can be approximated by

$$\bar{u}^{k+1} = \frac{A^\top (w^k - b_1^k) + \nabla^\top (q^k - b_2^k)}{A^\top A + \nabla^\top \nabla} \quad (4.8)$$

followed by one projection step

$$u_i^{k+1} := \frac{\sum_{j=1}^n f_j}{\sum_{j=1}^n \max(\bar{u}_j^{k+1}, 0)} \max(\bar{u}_i^{k+1}, 0), \quad \text{for } i = 1, \dots, n, \quad (4.9)$$

to ensure that u^{k+1} is nonnegative and preserves the mean of f . As the objective function of (4.3) corresponds to a typical singly linearly constrained quadratic programming problem subject to upper and lower bounds, we could also solve for the u^{k+1} by the algorithm proposed in Ref. [19]. However, in numerical experiments it has been found that this method is very time consuming, and produces almost identical results compared with formulae (4.8) and (4.9). In addition, the inexact Split-Bregman approach has previously produced quite good results [35], so here we calculate the u^{k+1} according to the formulae (4.8) and (4.9). In (4.4), the minimisation problem is strictly convex and involves the second derivative, but it can be solved efficiently by the Newton method with a projection. In our numerical experiments, we use four Newton iterations to calculate w^2 , and then only one Newton iteration to obtain w^{k+1} with $k > 2$. The solution of (4.5) can readily be obtained by applying the soft thresholding operator (cf. Ref. [15] for relevant properties) — i.e.

$$q^{k+1} = T_{\lambda\gamma}(b_2^k + \nabla u^{k+1}, \lambda\gamma),$$

where the soft thresholding operator is defined as

$$T_\tau(t) = \max(\|t\| - \tau, 0) \frac{t}{\|t\|},$$

with $t \in \mathbb{R}^{2n}$, $\|t\| = (|t_1|_2, \dots, |t_n|_2, |t_1|_2, \dots, |t_n|_2)^\top \in \mathbb{R}^{2n}$ involving $|t_i|_2 = \sqrt{t_i^2 + t_{i+n}^2}$ for $i = 1, \dots, n$ and the multiplication and division are point-wise.



Figure 1: Original images. (a) "Cameraman", (b) "Lena", (c) "Man".

5. Numerical Results

We compare the image restoration capabilities and CPU-time needed for our method with: (1) the method proposed in Ref. [2] for solving the AA model (1.4); (2) the method in Ref. [38] for solving the RLO model (1.2); and (3) the method in Ref. [43] for solving the KL-TV model (2.2). We recall that the AA model, the RLO model and our new model are all capable of deblurring simultaneously with multiplicative noise. The original grey level test images "Cameraman (256 × 256)", "Lena (512 × 512)" and "Man (512 × 512)" considered are shown in Fig. 1. The quality of the restoration results is compared quantitatively by means of the peak signal-to-noise ratio (PSNR), which is a widely used image quality assessment measure [8]. All simulations described here were run in Matlab 7.14 (R2012a) on a Dell PC Optiplex 9010.

In all of the numerical tests, we set the degraded image $f \geq 1$. For the AA model and the RLO model, we used the time-marching algorithm to solve the corresponding minimisation problem or its Lagrangian with multiplier λ , as proposed in Refs. [2, 38]. We set the step size to be 0.1 to ensure a stable iterative procedure, and the algorithms were stopped when a maximum number of iterations was reached. In addition, for all of the AA, RLO model and KL-TV models we adjusted the parameter λ through numerical tests until the largest PSNR values were reached. Based on Proposition 2.1 and 3.1, in order to obtain a convex model in our new hybrid method we set $\alpha = 1$ for all numerical simulations. Furthermore, the parameter γ in (4.2) was set at 50, which is critical [23, 41]. Moreover, we stopped our iterative procedure as soon as the value of the objective function no longer showed a big relative decrease — i.e. when

$$\frac{\|u^{k+1} - u^k\|_2}{\|u^{k+1}\|_2} < \varepsilon .$$

In all tests, we set $\varepsilon = 10^{-4}$ and tuned the parameter λ was empirically.

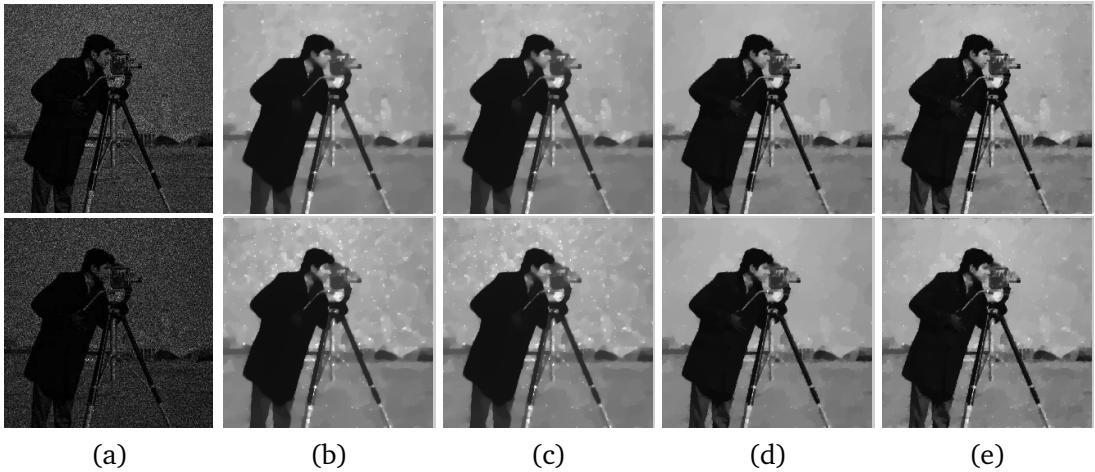


Figure 2: Results from different methods when restoring "Cameraman" corrupted by multiplicative noise where $K = 10$ (first row) and $K = 6$ (second row), respectively: (a) noisy images; (b) AA model; (c) RLO model; (d) KL-TV model; (e) our method.



Figure 3: Results from different methods when restoring "Lena" corrupted by multiplicative noise for $K = 10$ (first row) and $K = 6$ (second row), respectively: (a) noisy images; (b) AA model; (c) RLO model; (d) KL-TV model; (e) our method.

5.1. Image denoising

Although our hybrid method is intended to deal with the simultaneous deblurring and denoising of images subject to multiplicative noise, we first show that it can provide very good results for the noise removal alone. In the example, the test images are corrupted by multiplicative noise with $K = 10$ and $K = 6$, respectively. The results are shown in Figs. 2–4.

We chose to use $\lambda = 0.18$ for the noise level $K = 10$ and $\lambda = 0.21$ for the noise level $K = 6$, for both of the AA and RLO models; and for the KL-TV model, we set $\lambda = 0.35$ for

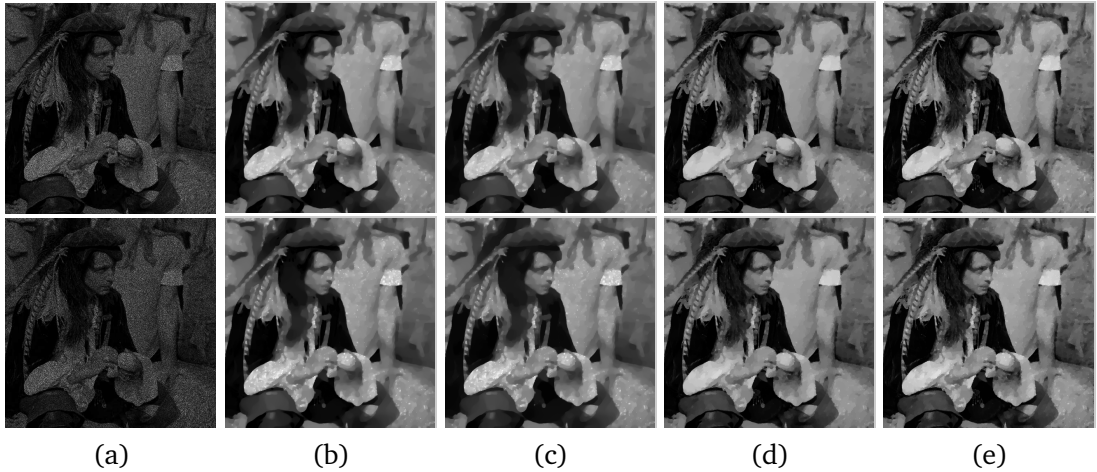


Figure 4: Results from different methods when restoring “Man” corrupted by multiplicative noise for $K = 10$ (first row) and $K = 6$ (second row), respectively: (a) noisy images; (b) AA model; (c) RLO model; (d) KL-TV model; (e) our method.

Table 1: Comparison of PSNR values in dB, the number of iterations, and the CPU-time in seconds, using the four different models for denoising.

		$K = 10$			$K = 6$		
		PSNR	k	Time	PSNR	k	Time
Cameraman	AA	24.27	3000	7.72	23.24	3000	7.77
	RLO	24.20	3000	33.34	23.16	3000	31.47
	KL-TV	25.64	200	2.26	24.60	200	2.37
	Ours	25.96	58	1.29	24.81	60	1.47
Lena	AA	27.12	3000	58.87	25.78	3000	60.23
	RLO	27.10	3000	156.14	25.75	3000	157.19
	KL-TV	28.35	200	17.04	27.29	200	16.61
	Ours	28.48	59	6.94	27.39	61	7.64
Man	AA	25.03	3000	59.14	24.40	3000	59.64
	RLO	24.87	3000	158.73	24.21	3000	155.86
	KL-TV	26.50	200	16.77	25.66	200	16.61
	Ours	26.96	56	6.69	26.01	58	7.04

$K = 10$ and $\lambda = 0.45$ for $K = 6$. For our model, we set $\lambda = 0.3$ and $\lambda = 0.4$ for the noise levels $K = 10$ and $K = 6$, respectively. As shown in Figs. 2–4, we found that much more noise remains in the restored images from the AA and RLO models compared to our model. The contrast details from the AA and RLO models are also noticeably reduced because of over-smoothing during noise removal. The KL-TV model produces better results than the AA and RLO models — some high-level noise is still visible, but especially there it does preserve more detail (cf. the tripod in “Cameraman” and the hat in “Lena”). To further compare recovery detail, in Fig. 4 we show the results for denoising the highly detailed image “Man”. Comparing the textures surrounding the hat and hair, it is clear that our method suppresses noise successfully while preserving significant details.

To compare performance and computational efficiency, in Table 1 we list the PSNR values of the restored results, the number of iterations required, and CPU-times. We observe

Table 2: Comparison of PSNR values in dB, the number of iterations, and the CPU-time in seconds, using three different models for deblurring with denoising.

		Motion Blur			Gaussian Blur			Uniform Blur		
		PSNR	k	Time	PSNR	k	Time	PSNR	k	Time
Camera-man	AA	21.74	10^4	24.54	21.38	10^4	24.09	20.82	10^4	23.96
	RLO	21.69	10^4	107.66	21.38	10^4	107.86	20.80	10^4	107.42
	Ours	22.45	89	2.45	22.65	110	2.73	22.19	109	2.64
Lena	AA	25.79	10^4	196.22	25.55	10^4	196.75	24.97	10^4	195.45
	RLO	25.72	10^4	511.90	25.47	10^4	514.63	24.98	10^4	514.71
	Ours	26.80	82	11.50	26.83	93	13.46	26.29	98	13.70
Man	AA	23.44	10^4	190.13	23.23	10^4	190.35	22.66	10^4	193.35
	RLO	23.40	10^4	506.80	23.17	10^4	510.06	22.59	10^4	507.53
	Ours	24.13	82	12.00	24.42	107	14.52	23.93	100	14.54

that the PSNR values from our method are more than 1 dB higher than those from the AA and RLO models. Moreover, our method is seen to produce consistently higher PSNR values than the KL-TV model. In addition, to obtain a stable iterative procedure the numerical solution methods for the AA and RLO models require a small step size, so some 3000 iterations were needed to provide the results with the best PSNR values. Although the numerical method to solve the KL-TV model requires rather less iterations, some 200 iterations were still needed to guarantee large PSNR values. However, with the split-Bregman algorithm used in our method, the stopping rule is satisfied after only around 60 iterations and better restored results are obtained. Furthermore, on comparing CPU-times our method is much more efficient than the other three methods. For example, when restoring the image ‘‘Lena’’ corrupted by multiplicative noise with noise level $K = 6$, the numerical methods for solving the AA, RLO and KL-TV models take 16, 25 and 3 times more CPU-time than our method, respectively. Moreover, the approach in Ref. [28] provides even better PSNR values, since it learns a ‘‘hidden dictionary’’ from noisy image patches.

5.2. Image deblurring and denoising

Let us now focus on restoring blurred images with multiplicative noise. In our numerical tests, we consider three different blurring operators — viz. motion blur with length 5 and angle 30, Gaussian blur with a window size 7×7 and a standard deviation of 2, and uniform blur with a window size 7×7 . Further, after blurring the test images are then corrupted by multiplicative noise with $K = 10$. In these tests, we set $\lambda = 0.05$ in the numerical methods used to solve the AA and RLO models, and $\lambda = 0.2$ in our method.

Figs. 5-7 show the degraded images and restored results for all three methods; and in Table 2 we list the PSNR values, the number of iterations, and the CPU-times. It is clear that our method gives the best PSNR values with the least iterations and CPU-times, for all images and blurring operators. Moreover, our method removes the noise successfully and preserves more details — cf. the tripod in ‘‘Cameraman’’ and the hats in ‘‘Lena’’ and ‘‘Man’’, for example. In summary, our method turns out to be more efficient and outperforms the other methods that handle deblurring, while simultaneously removing multiplicative noise.

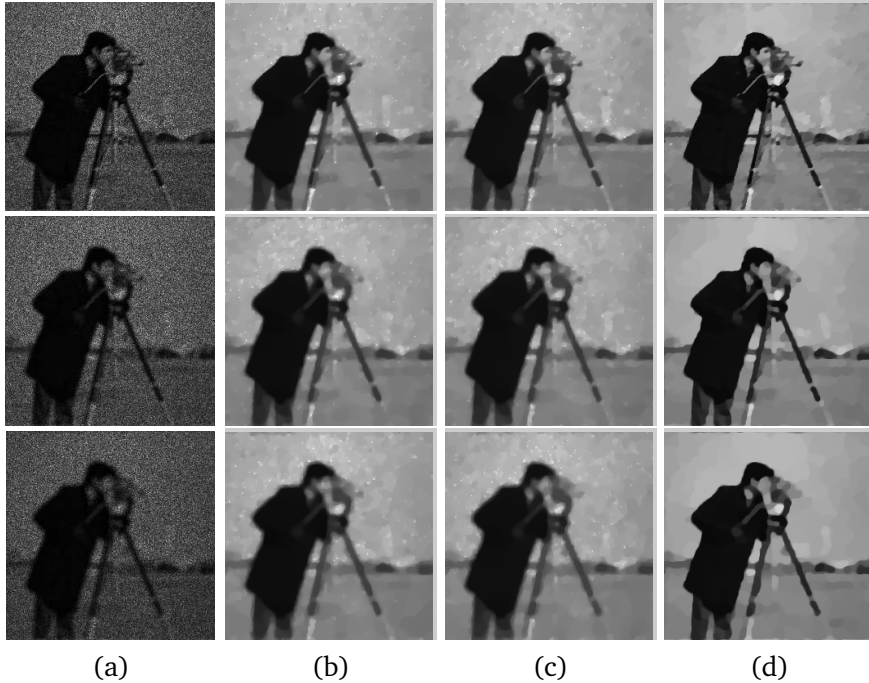


Figure 5: Results from three different methods for restoring the degraded “Cameraman” image, corrupted by multiplicative noise with $K = 10$ and motion blur (first row), Gaussian blur (second row), or uniform blur (third row). (a) Degraded images; (b) AA model; (c) RLO model; (d) our method.

6. Conclusion

We have proposed a new convex variational model for restoring images corrupted by blurring operators and multiplicative Gamma noise. The classical model for this task is non-convex, when the restoration is strongly dependent on the initialisation and numerical optimisation procedures. In order to overcome this difficulty, given previous work on multiplicative noise removal we combine MAP analysis of the Gamma distribution and I-divergence, in introducing our hybrid model that we have proven to be convex under a certain condition. In addition, we have investigated some important properties of this new model, such as the maximal principle and bias correction. To enhance our overall method, the split-Bregman algorithm was applied to solve the constrained minimisation problem in our hybrid model. Numerical results show that our method outperforms several recently proposed methods, both visually and quantitatively. Furthermore, the CPU-time consumed by our method is significantly less.

7. Acknowledgments

This work is supported by RGC 211710, RGC 211911 of the Research Grants Council, Hong Kong; and by the National Science Foundation of China (11271049).

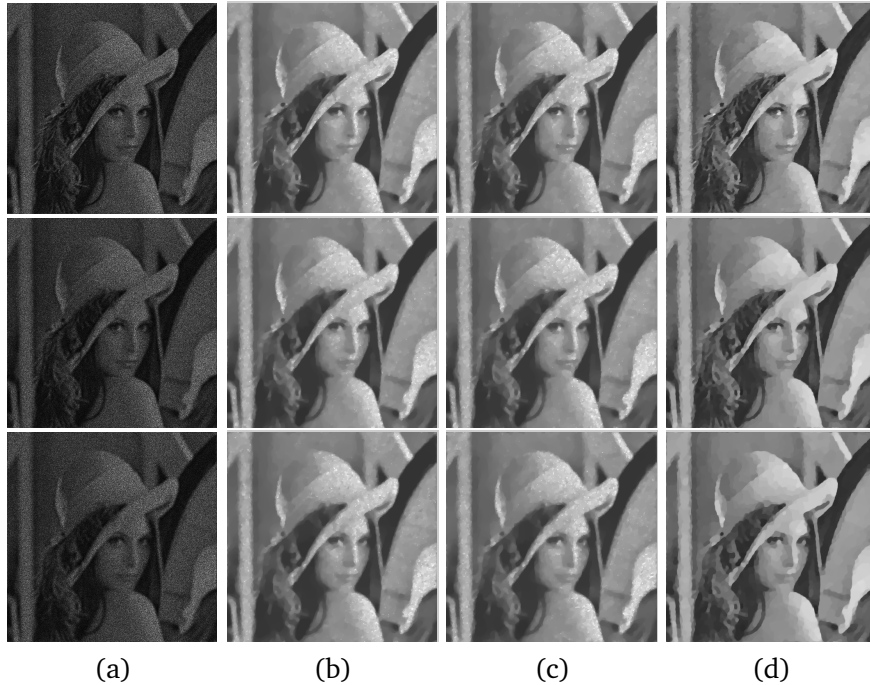


Figure 6: Results from three different methods for restoring the degraded “Lena” image, corrupted by multiplicative noise with $K = 10$ and motion blur (first row), Gaussian blur (second row), or uniform blur (third row). (a) Degraded images; (b) AA model; (c) RLO model; (d) our method.

References

- [1] L. Ambrosio, N. Fusco and D. Pallara, *Functions of Bounded Variation and Free Discontinuity Problem*, Oxford University Press (2000).
- [2] G. Aubert and J. Aujol, *A variational approach to removing multiplicative noise*. SIAM J. Appl. Math. **68**, 925–946 (2008).
- [3] G. Aubert and P. Kornprobst, *Mathematical Problems in Image Processing: Partial Differential Equations and the Calculus of Variations*, volume 147, Springer Verlag (2006).
- [4] M. Bertero, P. Boccacci, G. Desiderà and G. Vicidomini, *Image deblurring with Poisson data: from cells to galaxies*, Inverse Problems **25**, 123006 (2009).
- [5] J. Bioucas-Dias and M. Figueiredo, *Multiplicative noise removal using variable splitting and constrained optimisation*, IEEE Trans. Image Process. **19**, 1720–1730 (2010).
- [6] S. Bonettini and V. Ruggiero, *An alternating extra gradient method for total variation based image restoration from Poisson data*, Inverse Problems **27**, 095001 (2011).
- [7] S. Bonettini and V. Ruggiero, *On the convergence of primal-dual hybrid gradient algorithms for total variation image restoration*, J. Math. Imaging Vis. **44**, 236–253 (2012).
- [8] A. Bovik, *Handbook of Image and Video Processing*, Academic Press (2000).
- [9] S. Boyd, N. Parikh, E. Chu, B. Peleato and J. Eckstein, *Distributed optimisation and statistical learning via the alternating direction method of multipliers*, Found. Trends Mach. Learning **3**, 1–122 (2010).
- [10] L. Bregman, *The relaxation method of finding the common point of convex sets and its application to the solution of problems in convex programming*, USSR Comput. Math. Math. Phys. **7**, 200–217 (1967).

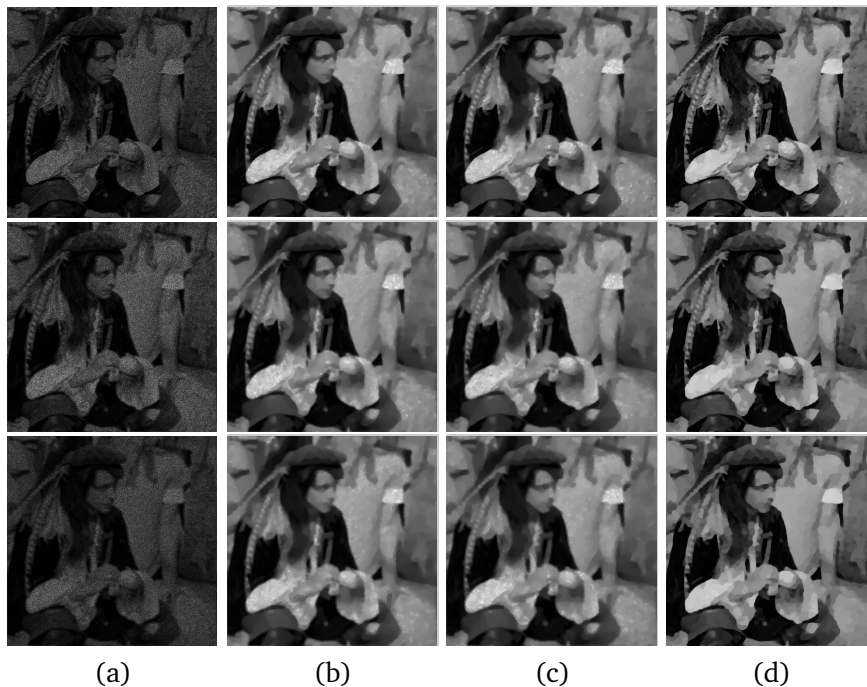


Figure 7: Results from different methods for restoring the degraded “Man” image, corrupted by multiplicative noise with $K = 10$ and motion blur (first row), Gaussian blur (second row), or uniform blur (third row). (a) Degraded images; (b) AA model; (c) RLO model; (d) our method.

- [11] J. Cai, R. Chan and Z. Shen, *A framelet-based image inpainting algorithm*, *Appl. Comput. Harmon. Anal.* **24**, 131–149 (2008).
- [12] A. Chambolle, *An algorithm for total variation minimisation and application*, *J. Math. Imaging Vis.* **20**, 89–97 (2004).
- [13] A. Chambolle and P. Lions, *Image recovery via total variation minimisation and related problems*, *Num. Mathematik* **76**, 167–188 (1997).
- [14] A. Chambolle and T. Pock, *A first-order primal-dual algorithm for convex problems with applications to imaging*, *J. Math. Imaging Vis.* **40**, 120–145 (2011).
- [15] T. Chan and J. Shen, *Image Processing And Analysis: Variational, PDE, Wavelet, and Stochastic Methods*, SIAM (2005).
- [16] C. Chaux, J. Pesquet and N. Pustelnik, *Nested iterative algorithms for convex constrained image recovery problems*, *SIAM J. Imaging Sci.* **2**, 730–762 (2009).
- [17] P. Combettes and J. Pesquet, *A Douglas-Rachford splitting approach to nonsmooth convex variational signal recovery*, *IEEE J. Selected Topics in Signal Processing* **1**, 564–574 (2007).
- [18] I. Csiszár, *Why least squares and maximum entropy? An axiomatic approach to inference for linear inverse problems*, *Ann. Statist.* **19**, 2032–2066 (1991).
- [19] Y. Dai and R. Fletcher, *New algorithms for singly linearly constrained quadratic programs subject to lower and upper bounds*, *Math. Program. A* **106**, 403–421 (2006).
- [20] S. Durand, J. Fadili and M. Nikolova, *Multiplicative noise removal using l_1 fidelity on frame coefficients*, *J. Math. Imaging Vis.* **36**, 201–226 (2010).
- [21] E. Esser, *Applications of Lagrangian-based alternating direction methods and connections to split Bregman*, CAM report 09-31, UCLA (March 2009).

- [22] E. Esser, X. Zhang and T. Chan, *A general framework for a class of first order primal-dual algorithms for convex optimisation in imaging science*, SIAM J. Imaging Sci. **3**, 1015–1046 (2010).
- [23] M. Figueiredo and J. Bioucas-Dias, *Restoration of Poissonian images using alternating direction optimisation*, IEEE Trans. Image Process. **19**, 3133–3145 (2010).
- [24] G. Gilboa and S. Osher, *Nonlocal operators with applications to image processing*, Multiscale Model. Sim. **7**, 1005–1028 (2009).
- [25] E. Giusti, *Minimal Surfaces and Functions of Bounded Variation* Birkhäuser, Boston (1984).
- [26] T. Goldstein and S. Osher, *The split Bregman method for l_1 regularized problems*, SIAM J. Imaging Sci. **2**, 323–343 (2009).
- [27] G. Grimmett and D. Welsh, *Probability: An Introduction*, Oxford Science Publications (1986).
- [28] Y. Huang, L. Moisan, M. Ng and T. Zeng, *Multiplicative noise removal via a learned dictionary*, IEEE Trans. Image Process. **21**, 4534–4543 (2012).
- [29] Y. Huang, M. Ng and Y. Wen, *A new total variation method for multiplicative noise removal*, SIAM J. Imaging Sci. **2**, 20–40 (2009).
- [30] Y. Huang, M. Ng and T. Zeng, *The convex relaxation method on deconvolution model with multiplicative noise*, Commun. Comput. Phys. **13**, 1066–1092 (2013). Source: <http://www.math.hkbu.edu.hk/~zeng/CiCp-MultiResto2012.pdf>.
- [31] S. Kontogiorgis and R. Meyer, *A variable-penalty alternating directions method for convex optimisation*, Math. Prog. **83**, 29–53 (1998).
- [32] P. Kornprobst, R. Deriche and G. Aubert, *Image sequence analysis via partial differential equations*, J. Math. Imaging Vis. **11**, 5–26 (1999).
- [33] S. Lintner and F. Malgouyres, *Solving a variational image restoration model which involves L^∞ constraints*, Inverse Problems **20**, 815–831 (2004).
- [34] T. Le, R. Chartrand and T. Asaki, *A variational approach to reconstructing images corrupted by Poisson noise*, J. Math. Imaging Vis. **27**, 257–263 (2007).
- [35] M. Ng, F. Wang and X. Yuan, *Inexact alternating direction methods for image recovery*, SIAM J. Sci. Comp. **33**, 1643–1668 (2011).
- [36] J. Nocedal and S. Wright, *Numerical Optimisation*, Springer Verlag (2006).
- [37] T. Pock, D. Cremers, H. Bischof, D. Cremers and A. Chambolle, *An algorithm for minimising the Mumford-Shah functional*, in Proc. 12th IEEE Int'l Conf. Computer Vision, pp. 1133–1140 (2009).
- [38] S. Osher and N. Paragios, *Multiplicative denoising and deblurring: theory and algorithms*, in *Geometric Level Set Methods in Imaging, Vision, and Graphics*, pp. 103–119, Springer Verlag (2003).
- [39] L. Rudin, S. Osher and E. Fatemi, *Nonlinear total variation based noise removal algorithms*, Physica D **60**, 259–268 (1992).
- [40] S. Setzer, *Operator splittings, Bregman methods and frame shrinkage in image processing*, Int. J. Comput. Vis. **92**, 265–280 (2011).
- [41] S. Setzer, G. Steidl and T. Teuber, *Deblurring Poissonian images by split Bregman techniques*, J. Visual Comm. Image Repres. **21**, 193–199 (2010).
- [42] J. Shi and S. Osher, *A nonlinear inverse scale space method for a convex multiplicative noise model*, SIAM J. Imaging Sci. **1**, 294–321 (2008).
- [43] G. Steidl and T. Teuber, *Removing multiplicative noise by Douglas-Rachford splitting methods*, J. Math. Imaging Vis. **36**, 168–184 (2010).
- [44] T. Teuber and A. Lang, *Nonlocal filters for removing multiplicative noise*, in A. M. Bruckstein et al. (Eds.) *Scale Space and Variational Methods in Computer Vision*, Third International Conference, SSVM 2011, pp. 50–61, Springer Verlag (2012).

- [45] C. Wu and X. Tai, *Augmented Lagrangian method, dual methods and split-Bregman iterations for ROF, vectorial TV and higher order*, SIAM J. Imaging Sci. **3**, 300–339 (2010).
- [46] T. Zeng and M. Ng, *On the total variation dictionary model optimisation*, IEEE Trans. Image Process. **19**, 821–825 (2010).
- [47] X. Zhang, M. Burger, X. Bresson and S. Osher, *Bregmanized nonlocal regularisation for deconvolution and sparse reconstruction*, SIAM J. Imaging Sci. **3**, 253–276 (2010).